Simultaneous Measurement of Spatial Room Impulse Responses from Multiple Sound Sources Using a Continuously Moving Microphone

Nara Hahn and Sascha Spors
Institute of Communications Engineering, University of Rostock, Germany
Email: nara.hahn@uni-rostock.de

***Abstract*—Continuous measurement techniques aim at identifying a large number of impulse responses from a signal captured by a moving microphone. In a recently proposed method, each sample of the captured signal is interpreted as a spatio-temporal sample of the sound field, and the individual impulse responses are computed by means of spatial interpolation. In the present study, the approach is extended towards multichannel cases. The superimposed sound field reproduced by multiple sources is recorded with one microphone, and the individual impulse responses are identified. To this end, the sound sources are excited with the same periodic perfect sequence, but a different amount of temporal shift is applied so that the identified impulse responses of different sources do not overlap. An anti-aliasing condition for the microphone speed is derived which is computed based on the spatial bandwidth of the sound field.**

I. Introduction

One of the recent trends in virtual acoustics is the analysis and synthesis of sound fields with high spatial fidelity. Binaural synthesis is employing head-related transfer function (HRTF) data sets that cover all possible source directions as well as head orientations [1]. Also, an increasing number of loudspeakers are used in multichannel sound reproduction systems in order to achieve high physical and/or perceptual resolution [2]. This accompanies the need for capturing sound fields with rich spatial information, thus requiring a large number of measurements, such as sound field recordings or spatial impulse responses [3, 4].

Continuous measurement techniques are capable of acquiring a large number of impulse responses by using a moving microphone [5–8]. These methods are particularly useful if the impulse responses are measured at densely distributed receiver positions. Typically, the acoustic system is excited periodically by a signal exhibiting a perfect auto-correlation property. The microphone passes through all the desired receiver positions, and captures the reproduced sound field. The impulse responses are then extracted from the microphone signal, which constitutes an off-line time-varying system identification approach.

The authors introduced a continuous measurement technique [7], where the captured signal is interpreted as spatio-temporally sampled from the sound field, and the impulse responses are computed by means of spatial interpolation. The method was applied to practical measurements, e.g. spatial room impulse response and binaural room impulse response measurement [9, 10]. The present paper extends the method to the multichannel case, where more than one sound source is driven simultaneously and the superimposed sound field is captured by one microphone. In order to avoid overlap of the impulse responses from different sources, different time-shifts are applied to the source signals. This approach is adopted from [11, 12] where adaptive filters are used for time-varying system identification.

The remainder of this paper is organized as follows. The continuous measurement method using spatial interpolation is introduced in Sec. II. It is extended to the multiple-source case in Sec. III including a modified spatial anti-aliasing condition. The presented method is evaluated in Sec. IV by numerical simulations.

Nomenclature Discrete-time signals and digital filter coefficients in the time-domain are denoted by lower case $h(n)$ with n denoting the discrete-time index. The corresponding discrete Fourier transform (DFT) is denoted by upper case, $H(\mu)$ where μ denotes the frequency index. Position vectors are denoted by boldface lower case $\mathbf{x}$. The imaginary unit is denoted by i, and the speed of sound by c.

II. Continuous Measurement

For the identification of a linear time-invariant system, a sound source at position $\mathbf{x}'$ is driven by an excitation signal $\psi(n)$. The sound field at $\mathbf{x}$ is represented by a finite impulse response (FIR) model,

$$p(\mathbf{x}, n) = \sum_{k=0}^{N_h-1} \psi(n-k) h(\mathbf{x}, \mathbf{x}', k), \tag{1}$$

where $p(\mathbf{x}, n)$ denotes the sound field and $h(\mathbf{x}, \mathbf{x}', k)$ the corresponding impulse response. The length of the impulse response is assumed to N_h samples.

A. Excitation by Perfect Sequence

For the continuous measurement, an N-periodic signal is used that satisfies the perfect auto-correlation property,

$$\mathring{\rho}_{\psi\psi}(k) \equiv \sum_{n=0}^{N-1} \psi(n)\psi(n-k) = \|\psi\|^2 \cdot \delta(k \bmod N), \tag{2}$$

where $\mathring{\rho}_{\psi\psi}(k)$ denotes the circular auto-correlation of $\psi(n)$ and $\|\psi\| \equiv \left[\sum_{n=0}^{N-1} |\psi(n)|^2\right]^{1/2}$ the norm of the respective

ISBN 978-90-827970-1-5

signal. Since $\delta(n)$ denotes the unit impulse, $\delta\left(k \bmod N\right)$ is an impulse train. Such a finite-length sequence, called perfect sequence, is preferred in system identification, since it excites all the orthogonal components of a system within a period [13], provided that $N > N_h$ [14]. In the frequency domain, the perfect auto-correlation property (2) is represented as

$$|\Psi(\mu)|^2 \equiv \Psi(\mu)\Psi(\mu)^* = \|\psi\|^2, \tag{3}$$

for $\mu = 0, 1, \ldots, N-1$, where $\Psi(\mu)$ denotes the length-N DFT of $\psi(n)$ and $(\cdot)^*$ the complex conjugate. Therefore, any finite-length sequence having the spectrum

$$\Psi(\mu) = \frac{1}{\|\psi\|} e^{i\alpha(\mu)} \tag{4}$$

is a perfect sequence if the phase $\alpha(\mu)$ is real-valued. Without loss of generality, $\|\psi\| = 1$ is assumed in the remainder.

Once the system is periodically excited by a perfect sequence $\psi(n)$, the sound field $p(\mathbf{x}, n)$ becomes periodic with the same period N. Due to property (2), the impulse response at position $\mathbf{x}$ is obtained from the length-N circular cross-correlation of $p(\mathbf{x}, n)$ and $\psi(n)$,

$$h(\mathbf{x}, \mathbf{x}', n) = \mathring{\rho}_{p\psi}(n) \equiv \sum_{k=0}^{N-1} p(\mathbf{x}, k)\psi(k-n), \tag{5}$$

for $n = 0, 1, \ldots, N_h$. Notice that, if $N > N_h$, the circular cross-correlation $\mathring{\rho}_{p\psi}(n)$ is a zero-padded version of the original impulse response, therefore, the last $N - N_h$ samples can be discarded.

B. Spatial Sampling

Assume that an omni-directional microphone moves on a trajectory represented by $\tilde{\mathbf{x}}(n)$. The captured signal reads

$$s(n) = p\left(\tilde{\mathbf{x}}(n), n\right), \tag{6}$$

which constitutes a sampling of the sound field in time and space. Considering the N-periodicity of the sound field, the captured samples can be grouped into N disjoint sets based on the value of $n \bmod N$,

$$\begin{aligned}
\mathcal{S}_0 &= \Big\{ s(0), s(N), s(2N), \ldots \Big\}, \\
\mathcal{S}_1 &= \Big\{ s(1), s(N+1), s(2N+1), \ldots \Big\}, \\
&\vdots \\
\mathcal{S}_{N-1} &= \Big\{ s(N-1), s(2N-1), s(3N-1) \ldots \Big\}.
\end{aligned} \tag{7}$$

By exploiting (6), the elements of the ν-th set $\mathcal{S}_\nu$ can be rewritten as

$$\Big\{ p\left(\tilde{\mathbf{x}}(\nu), \nu\right), p\left(\tilde{\mathbf{x}}(\nu+N), \nu\right), p\left(\tilde{\mathbf{x}}(\nu+2N), \nu\right), \ldots \Big\}. \tag{8}$$

Although not captured simultaneously, those samples can be interpreted as spatially sampled from the sound field at the same moment $n = \nu$. Denoting the length of the captured signal by L, the sound field is sampled at $\frac{L}{N}$ different positions for each n. In the context of continuous measurement, the latter is considered as the effective number of spatial sampling points [9].

C. Spatial Interpolation

The next step is to reconstruct the original sound field at the desired position by using spatial interpolation. The interpolation is performed for each set $\mathcal{S}_n$ in (7),

$$\hat{p}\left(\mathbf{x}, n\right) = \mathcal{L}\left(\mathcal{S}_n\right), \quad n = 0, 1, \ldots, N-1, \tag{9}$$

where $\mathcal{L}$ denotes the interpolation operator and $\hat{(\cdot)}$ an estimate of the respective variable. Finally, the impulse response is given as the circular cross-correlation of $\hat{p}(\mathbf{x}, n)$ and $\psi(n)$,

$$\hat{h}\left(\mathbf{x}, \mathbf{x}', n\right) = \mathring{\rho}_{\hat{p}\psi}(n) = \sum_{k=0}^{N-1} \hat{p}\left(\mathbf{x}, k\right) \psi(k-n). \tag{10}$$

As pointed out in [15], the interpolator in (9) should be chosen carefully by taking the spatial distribution of the sampling points into account.

III. Multiple-Source Case

This section considers the continuous measurements for multiple sound sources. The positions of M sources are denoted by

$$\mathbf{x}'_0,\ \mathbf{x}'_1,\ \ldots,\ \mathbf{x}'_{M-1}, \tag{11}$$

where the subscripts indicate the source indices. The goal is to acquire the impulse responses of multiple sources at multiple receiver positions. Since only one microphone is used, the time-invariant multiple-input/multiple-output (MIMO) system is identified using a time-varying multiple-input/single-output (MISO) system.

A. Excitation by Multiple Perfect Sequences

In order to cope with the interference between different sources, an approach similar to [12, Sec. 7.3] is employed. While each source is driven by the same perfect sequence, a temporal shift of $m \times N_h$ is applied to the m-th source,

$$\psi(n - mN_h) \quad \text{for } m = 0, 1, \ldots, M-1. \tag{12}$$

The sound fields produced by the individual sources are superimposed resulting in

$$\begin{aligned}
p(\mathbf{x}, n) &= \sum_{m=0}^{M-1} \sum_{k=0}^{N_h-1} \psi(n - mN_h - k) h(\mathbf{x}, \mathbf{x}'_m, k) \\
&= \sum_{\kappa=0}^{N_h-1} \psi(n-\kappa) \Big[\sum_{m=0}^{M-1} h(\mathbf{x}, \mathbf{x}'_m, \kappa - mN_h) \Big],
\end{aligned} \tag{13}$$

where, in the second equality, k is replaced by $\kappa = k + mN_h$. Note that the period of $\psi(n)$ is still N. Equation (13) can be considered as the sound field of a single sound source driven by $\psi(n)$, where the notional source is composed of M spatially distributed components having internal delays. The corresponding impulse response is represented by the bracketed term $\left[\,\cdot\,\right]$, which is a shifted sum of the impulse responses of the M sources. Similar to the single-channel case,

ISBN 978-90-827970-1-5

the notional impulse response is obtained from the length-N circular cross-correlation of $p(\mathbf{x}, n)$ and $\psi(n)$,

$$\begin{aligned}\mathring{\rho}_{p\psi}(n) &= \sum_{l=0}^{N-1} p(\mathbf{x}, l)\psi(l-n) \\ &= \sum_{l=0}^{N-1} \psi(l-n) \sum_{k=0}^{N_h-1} \psi(l-k) \sum_{m=0}^{M-1} h(\mathbf{x}, \mathbf{x}'_m, k-mN_h) \\ &= \sum_{m=0}^{M-1} \sum_{k=0}^{N_h-1} h(\mathbf{x}, \mathbf{x}'_m, k-mN_h) \sum_{l=0}^{N-1} \underbrace{\psi(l-n)\psi(l-k)}_{\delta((k-n) \bmod N)} \\ &= \sum_{m=0}^{M-1} h(\mathbf{x}, \mathbf{x}'_m, n-mN_h), \end{aligned} \tag{14}$$

for $n = 0, 1, \ldots, N-1$. The individual impulse responses can be easily separated, if their non-zero parts do not overlap. Since M impulse responses have to fit in N samples, the perfect sequence must be longer than the concatenation of the impulse responses, i.e. $N \geq M \times N_h$.

B. Multichannel System Identification

The multi-channel system identification is now converted to a single-channel system identification where multiple systems are identified as a whole [12, Sec. 7.3]. Therefore, the system identification process is the same as described in Sec. II. The captured signal $s(\mathbf{x}, n)$ is interpreted as spatio-temporally sampled from the sound field, and the original sound field is estimated by spatial interpolation.

Once the sound field at the target position is computed, the m-th impulse response is obtained by shifting and windowing $\mathring{\rho}_{\hat{p}\psi}(n)$,

$$\hat{h}(\mathbf{x}, \mathbf{x}'_m, n) = \mathring{\rho}_{\hat{p}\psi}(n + mN_h) \times w(n), \tag{15}$$

where $w(n)$ denotes a rectangular window of length N_h,

$$w(n) = \begin{cases} 1, & n = 0, 1, \ldots, N_h - 1 \\ 0, & \text{otherwise.} \end{cases} \tag{16}$$

In practical implementations, an array of size N is obtained from (14), and the process of (15) is carried out by reshaping it into an $M \times N_h$ array.

C. Anti-aliasing Condition for Circular Trajectories

Before closing this section, an anti-aliasing condition is introduced which determines the maximum speed of the microphone for the continuous measurement on a circular trajectory. The microphone is assumed to move uniformly on a circle of radius r, which is located in the horizontal plane $z = z'$,

$$\tilde{\mathbf{x}}(n) = \left(r\cos\tilde{\phi}(n), r\sin\tilde{\phi}(n), z'\right). \tag{17}$$

The azimuth angle is denoted by $\tilde{\phi}(n) = \Omega \times \frac{n}{f_s}$ where Ω is the angular speed in rad/s. For a 2π-rotation, the effective number of sampling points is $\frac{2\pi}{\Omega}\frac{1}{N}f_s$. The spatial bandwidth is typically represented by the maximum order of a truncated circular harmonics expansion that reasonably approximates the sound field within a region of interest [4]. For a monochromatic sound field (frequency f) bounded on a circle, the spatial bandwidth is approximated by $\lceil \frac{2\pi f}{c} r \rceil$ [4, Sec. 4.2], where $\lceil \cdot \rceil$ denotes the ceiling function. This requires at least $2\lceil \frac{2\pi f}{c} r \rceil + 1$ sampling points on the circle. In order to avoid spatial aliasing, the parameters of the continuous measurement have to satisfy

$$\frac{2\pi}{\Omega}\frac{1}{N} f_s \geq 2\left\lceil \frac{2\pi f}{c} r \right\rceil + 1. \tag{18}$$

By arranging above equation with respect to Ω, the anti-aliasing angular speed $\Omega_{\text{al.}}$ is obtained,

$$\Omega \leq \Omega_{\text{al.}} = \frac{2\pi f_s}{N\left(2\left\lceil \frac{2\pi f}{c} r \right\rceil + 1\right)} \tag{19}$$

$$\leq \frac{2\pi f_s}{MN_h\left(2\left\lceil \frac{2\pi f}{c} r \right\rceil + 1\right)}. \tag{20}$$

This states that the speed of the microphone needs to be slowed down by a factor of M, which increases the measurement duration M times. This results in the same duration as for M repetitions of a single-channel measurement, if the preparation time between consecutive measurements is ignored. Even though, the multi-channel measurement has the practical advantage of reducing the noise and vibration caused by the moving parts, which usually increases with the speed of the microphone.

Note also that (20) holds only for uniformly moving microphones. For non-uniform movements, the resulting spatial distribution of the sampling points has to be taken into account, rather than the speed itself [16].

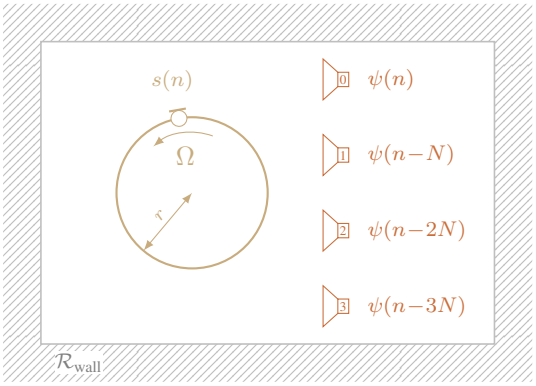

Fig. 1: Continuous measurement of the impulse responses of a 4-channel loudspeaker system in a rectangular room (reflection coefficient $\mathcal{R}_{\text{wall}}$). The m-th loudspeaker is driven by a time-shifted perfect sequence $\psi(n - mN)$. The sound field is captured by the microphone moving on the circle.

IV. Evaluation

The proposed method is evaluated by numerical simulations, where the impulse responses of multiple sources are identified.

A. Experimental Setup

The experimental set up is depicted in Fig. 1. The impulse responses of a rectangular room ($5.0 \times 5.9 \times 3.0$ m^3) are

ISBN 978-90-827970-1-5 © EURASIP 2018

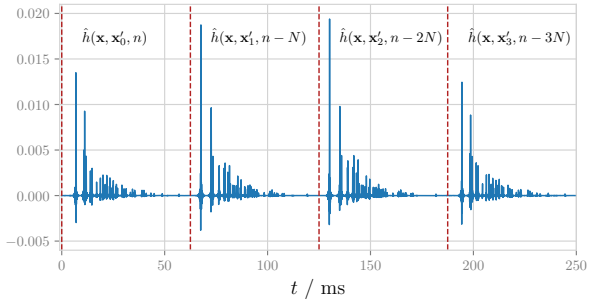

Fig. 2: Concatenation of the 4 impulse responses, which is the circular cross-correlation $\mathring{\rho}_{\hat{p}\psi}(n)$ ($\Omega = \frac{\pi}{10}$ rad/s, $\varphi_k = 0$, $N = 4000$, $N_h = 1000$). The vertical dashed lines indicate every 1000 samples.

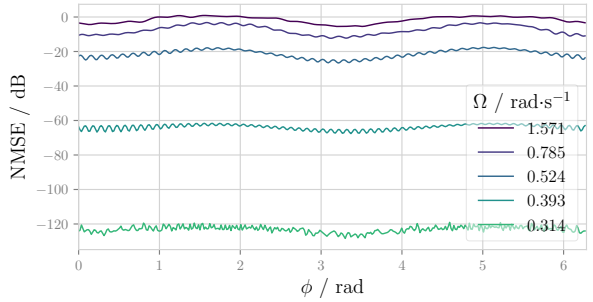

Fig. 3: NMSE of the sound source at $\mathbf{x}'_2$ for varying Ω.

simulated by using the image source method of 2nd-order, resulting in 1 direct sound and 24 reflections. Each component is modelled as a band-limited pulse (cut-off frequency 6.4 kHz). The reflection coefficients of all six walls are assumed to be frequency-independent and set to $\mathcal{R}_{\text{wall}} = 0.5$.

Four loudspeakers, modelled as point sources, are placed in the horizontal plane $z = 1.5$ m,

$$\mathbf{x}'_1 = (1.8, 1.8, 1.5), \qquad \mathbf{x}'_2 = (1.8, 1.0, 1.5)$$
$$\mathbf{x}'_3 = (1.8, -1.0, 1.5), \qquad \mathbf{x}'_4 = (1.8, -1.8, 1.5).$$

The goal is to obtain 4×360 impulse responses on a circle of radius $r = 0.2$ m centered at $(0,\ 0,\ 1.5)$. The target receiver positions are uniformly distributed on the circle with azimuth angles of

$$\varphi_k = 2\pi \times \tfrac{k}{360}, \quad \text{for } k = 0, 1, \ldots, 359. \tag{21}$$

For the continuous measurement, an omni-directional microphone is moved counter-clockwise on the circle with varying angular speeds,

$$\Omega = \tfrac{2\pi}{l}, \quad \text{for } l = 4, 6, \ldots, 20. \tag{22}$$

The signal captured by the microphone is simulated at a sampling frequency of 16 kHz. The propagation delay from the image sources to the receiver is implemented with fractional delay filters [17]. The speed of sound is set to $c = 343$ m/s.

The maximum distance from the farthest image source to the receivers is about 20.0 m, corresponding to 935 samples. Adding the half-lengths of the fractional delay filter and the low-pass filter for band-limitation leads to an impulse response length of 986 samples which is roughly approximated to be $N_h = 1000$. The 4 sound sources are thus driven by a perfect sequence of period $N = 4 \times N_h = 4000$. The pseudo-random perfect sequence is generated where $\alpha(\mu)$ in (4) exhibits a random phase in $[0, 2\pi)$.

From (20), the anti-aliasing condition for the measurement set up is $\Omega_{\text{al.}} \approx 0.513$ rad/s (29.4 °/s) corresponding to about 12 sampling points on the circumference. Therefore, a continuous measurement with $\Omega > \Omega_{\text{al.}}$ constitutes an under-sampling of the sound field, whereas a measurement with $\Omega < \Omega_{\text{al.}}$ an over-sampling.

The sound fields at the target positions are computed from the captured signal by using the periodic sinc interpolation. As shown in Fig. 2, the cross-correlation of the sound field and the excitation signal (14) gives the concatenation of the impulse responses. Since the excitation period N is properly chosen, the impulse responses do not overlap and can be separated as described in Sec. III.

B. Performance Measures

The difference between the desired and the measured impulse responses are quantified in terms of the normalized mean square error (NMSE) $\mathcal{E}_m(\varphi_k)$,

$$\mathcal{E}_m(\varphi_k) = \frac{\|\hat{h}_m(\varphi_k, n) - h_m(\varphi_k, n)\|}{\|h_m(\varphi_k, n)\|}, \tag{23}$$

where $\hat{h}_m(\varphi_k, n)$ denotes the identified impulse response of the m-th source at azimuth angle φ_k.

The similarity of $h_m(\varphi_k, n)$ and $\hat{h}_m(\varphi_k, n)$ is examined by the linear cross-correlation [9],

$$\rho^{(m)}_{h\hat{h}}(\varphi_k, n) = \tag{24}$$
$$\frac{1}{\|h_m\| \cdot \|\hat{h}_m\|} \sum_{k=-N_h+1}^{N_h-1} h_m(\varphi_k, k)\hat{h}_m(\varphi_k, k-n),$$

which is normalized by the energy of both impulse responses. The maximum of the cross-correlation $\gamma_m(\varphi_k) = \max\{\rho^{(m)}_{h\hat{h}}(\varphi_k, n)\}$ is interpreted as the similarity of the two waveforms, whereas the displacement of $\tau_m(\varphi_k) = \operatorname{argmax}_n\{\rho^{m}_{h\hat{h}}(\varphi_k, n)\}$ from 0 is interpreted as the temporal misalignment. For perfectly identical impulse responses, the former is equal to 1 and the latter to 0. Prior to the computation, the impulse responses are upsampled by a factor of 20, in order to increase the temporal resolution.

The overall performance of each continuous measurement is represented by the mean value of $\mathcal{E}_m(\varphi_k)$ and $\gamma_m(\varphi_k)$,

$$\bar{\mathcal{E}} = \langle\langle \mathcal{E}_m(\varphi_k)\rangle_k\rangle_m, \ \bar{\gamma} = \langle\langle \gamma_m(\varphi_k)\rangle_k\rangle_m, \tag{25}$$

where $\langle\cdot\rangle_{\{k,m\}}$ denotes the average over the respective variable. For the temporal misalignment, the unbiased standard deviation σ_τ is considered.

ISBN 978-90-827970-1-5

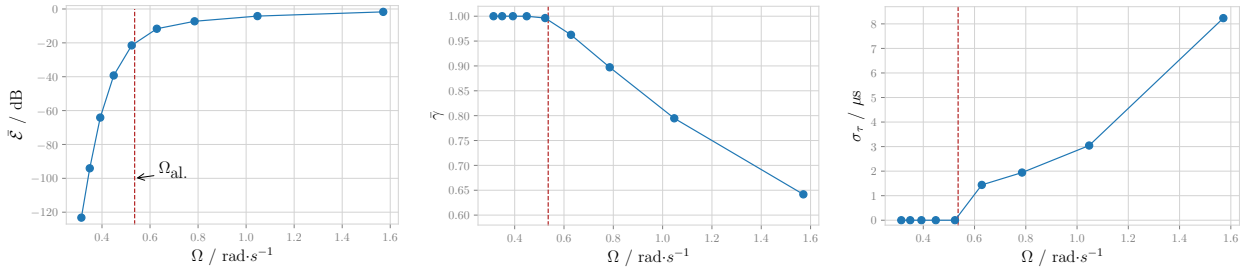

(a) NMSE $\bar{\mathcal{E}}$ (b) Waveform similarity $\bar{\gamma}$ (c) Temporal misalignment σ_τ

Fig. 4: Overall performance of the continuous measurements for varying Ω. The mean value of $\mathcal{E}_m(\varphi_k)$ and $\gamma_m(\varphi_k)$ are shown in (a) and (b), respectively. The standard deviation of $\tau_m(\varphi_k)$ is shown in (c).

C. Results

The NMSEs for source at $\mathbf{x}_2'$ are shown in Fig. 3. The angular speed is varied, $\Omega = \frac{2\pi}{4}, \frac{2\pi}{8}, \frac{2\pi}{12}, \frac{2\pi}{16}, \frac{2\pi}{20}$, which corresponds to the effective number of sampling points of $64, 128, 192, 256, 320$, respectively. In general, the NMSE gets slightly lower at the angles where the tangent of the microphone trajectory is perpendicular to the direction of the direct sound. This is attributed to the lower changing rate of the system in those regions, which eases the tracking of the system. Because of the reflections arriving from different directions, the angular dependency is less pronounced as observed in [18, Fig. 3(c)] and [15, Fig. 3] where free field conditions are considered. Although not shown here, the results for other sources are very similar, except the slightly different angular dependencies. The improvement for $\Omega < \Omega_{\text{al.}}$ is clearly seen, which validates the anti-aliasing condition (20).

The latter is more apparent from the overall performance, $\bar{\mathcal{E}}$, $\bar{\gamma}$, and σ_τ, shown in Fig. 4. All three performance measures confirm that the accuracy of the continuous measurement increases significantly for $\Omega < \Omega_{\text{al.}}$. Similar to the results in [15], the NMSE further decreases below $\Omega_{\text{al.}}$ due to the fact that the circular harmonic spectrum is not strictly band-limited. The waveforms of the impulse responses match almost perfectly in the over-sampling cases ($\Omega < \Omega_{\text{al.}}$). The largest time misalignment observed in the simulations is 8.2 μs which is about 0.13 times the sampling period (62.5 μs).

V. Conclusion

In this paper, the continuous measurement method based on spatial interpolation is extended to the multiple-source case. The individual sources are driven with time-shifted perfect sequences, which transforms the multichannel system identification problem into the conventional single-channel problem. Consequently, a concatenation of the impulse responses is obtained from which the individual impulse responses are easily separated. The anti-aliasing condition is derived which is adapted to the multiple-source case.

The results from numerical simulations are evaluated using three performance criteria, where the presented approach for multichannel system identification as well as the suggested anti-aliasing condition are verified. These must be further validated by real impulse response measurements, e.g. binaural room impulse responses of a multi-channel loudspeaker system.

Acknowledgment

This research was supported by a grant of the Deutsche Forschungsgemeinschaft (DFG) SP 1295/7-1.

References

[1] F. Brinkmann, A. Lindau, S. Weinzierl, M. Müller-Trapet, R. Opdam, M. Vorländer *et al.*, "A High Resolution and Full-Spherical Head-Related Transfer Function Database for Different Head-Above-Torso Orientations," *J. Audio Eng. Soc. (JAES)*, vol. 65, no. 10, pp. 841–848, 2017.

[2] S. Spors, H. Wierstorf, A. Raake, F. Melchior, M. Frank, and F. Zotter, "Spatial Sound with Loudspeakers and its Perception: A Review of the Current State," *IEEE Proc.*, vol. 101, no. 9, pp. 1920–1938, September 2013.

[3] B. Rafaely, *Fundamentals of Spherical Array Processing*. Springer, 2015.

[4] A. Kuntz, *Wave Field Analysis Using Virtual Circular Microphone Arrays*. München: Verlag Dr. Hut, 2009.

[5] T. Ajdler, L. Sbaiz, and M. Vetterli, "Dynamic Measurement of Room Impulse Responses Using a Moving Microphone," *J. Acoust. Soc. Am. (JASA)*, vol. 122, no. 3, pp. 1636–1645, 2007.

[6] C. Antweiler and M. Antweiler, "System Identification with Perfect Sequences based on the NLMS Algorithm," *AEU. Archiv für Elektronik und Übertragungstechnik*, vol. 49, no. 3, pp. 129–134, 1995.

[7] N. Hahn and S. Spors, "Identification of Dynamic Acoustic Systems by Orthogonal Expansion of Time-variant Impulse Responses," in *Proc. Int. Sym. Commun. Control Signal Process. (ISCCSP)*, Athens, Greek, May 2014.

[8] F. Katzberg, R. Mazur, M. Maass, P. Koch, and A. Mertins, "Measurement of Sound Fields Using Moving Microphones," in *Proc. of the 42nd IEEE Int. Conf. Acoust. Speech Signal Process. (ICASSP)*, New Orleans, USA, Mar. 2017.

[9] N. Hahn and S. Spors, "Continuous Measurement of Impulse Responses on a Circle Using a Uniformly Moving Microphone," in *Proc. Eur. Signal Process. Conf. (EUSIPCO)*, Nice, France, Aug. 2015.

[10] N. Hahn, W. Hahne, and S. Spors, "Dynamic Measurement of Binaural Room Impulse Responses Using an Optical Tracking System," in *Proc. Int. Conf. Spatial Audio (ICSA)*, Graz, Austira, Sep. 2017.

[11] C. Antweiler, A. Telle, and P. Vary, "NLMS-type System Identification of MISO Systems with Shifted Perfect Sequences," *Proc. Int. Workshop Acoust. Signal Enhancement (IWAENC)*, Sep. 2008.

[12] C. Antweiler, "Multi-Channel System Identification with Perfect Sequences," in *Advances in Digital Speech Transmission*. John Wiley & Sons, 2008, pp. 171–198.

[13] C. Antweiler and M. Dörbecker, "Perfect Sequence Excitation of the NLMS Algorithm and its Application to Acoustic Echo Control," *Annales Des Télécommunications*, vol. 49, no. 7, pp. 386–397, Jul. 1994.

[14] C. Antweiler and G. Enzner, "Perfect Sequence LMS for Rapid Acquisition of Continuous-azimuth Head Related Impulse Responses," in *Proc. IEEE Workshop Appl. Signal Process. Audio Acoust. (WASPAA)*, New Paltz, NY, USA, Oct. 2009.

[15] N. Hahn and S. Spors, "Spatial Aliasing in Continuous Measurement of Spatial Room Impulse Responses," in *Proc. German Annu. Conf. Acoust. (DAGA)*, Kiel, Germany, Mar. 2017.

[16] ——, "Continuous Measurement of Spatial Room Impulse Responses Using a Non-Uniformly Moving Microphone," in *Proc. IEEE Workshop Appl. Signal Process. Audio Acoust. (WASPAA)*, New Paltz, NY, USA, Oct. 2017.

[17] T. I. Laakso, V. Valimaki, M. Karjalainen, and U. K. Laine, "Splitting the Unit Delay," *IEEE Signal Process. Mag.*, vol. 13, no. 1, pp. 30–60, 1996.

[18] N. Hahn and S. Spors, "Comparison of Continuous Measurement Techniques for Spatial Room Impulse Responses," in *Proc. Eur. Signal Process. Conf. (EUSIPCO)*, Budapest, Hungary, Aug. 2016.